EXPERIMENTAL ANALYSIS OF DIFFERENT OPERATIONAL CONFIGURATIONS FOR SINGLE SIDED NATURAL VENTILATION AS PART OF A LOW ENERGY RETROFIT

Paul D O'Sullivan[*1, 2], Maria Kolokotroni [2]

1. *Department of Process, Energy & Transport, School of Mechanical Engineering, Cork Institute of Technology, Cork, Rossa Avenue, Bishopstown, Cork, Ireland*

2. *Howell Building, Mechanical Engineering, School of Engineering and Design, Brunel University, Uxbridge UB8 3PH, United Kingdom*

Corresponding author: paul.osullivan@cit.ie

ABSTRACT

Non-invasive, scalable, building retrofit solutions are amongst the most likely large scale adoption techniques to assist in climate change adaptation in the existing built environment, particularly in university type buildings where rehousing live activities will prove costly. Natural ventilation is an attractive retrofit strategy due to the low impact nature of the installation. A number of internal environmental criteria that are important to ventilative cooling strategies can be substantially modified as a result of an external retrofit solution. These include ventilation rate, internal thermal stratification, diurnal thermal stability, surface and air temperature variations etc. More generally, additional factors that can influence single sided natural ventilation performance related to the building microclimate are wind speed and direction, outdoor temperature profile, turbulent characteristics of the wind and pressure differences across the building envelope. This paper presents results from full scale performance testing of the natural ventilation system of a deep retrofit solution applied to an existing 1970s precast concrete building in south of Ireland. The solution presented is modular, scalable, externally applied and incorporates opaque and transparent elements as well as integrated automated and manual ventilation openings. The paper outlines different operational configurations for the single sided natural ventilation system and the respective effect these configurations have on internal environment based on full scale testing under dynamic outdoors conditions. Results are based on data collected for two single sided, direct gain cellular offices, one in the existing building that has not been retrofitted which acts as the control space, and the other one retrofitted to a very high standard. Four different types of ventilation configuration are summarised. The findings show that thermal stratification has been found to be substantially modified post retrofit although the relative magnitude is still significant in the retrofit due to reduced indoor temperatures while the amplitude of diurnal indoor air temperature has been effectively eliminated. The ventilation rate is also considerably lower in the retrofit spaces under some configurations. Each configuration is classified based on findings.

1   INTRODUCTION

Ventilative cooling coupled with exposed thermal mass is widely accepted as an important strategy for reducing summer overheating in non-domestic buildings. Extended monitoring has shown that naturally ventilated buildings typically use less than 50% of the corresponding energy consumption of air conditioned buildings and assessment of ventilative cooling techniques in Europe have shown they may contribute highly to reducing the cooling needs of buildings (Kolokotroni et al 1996a, 1996b; 2002) and be an effective tool for tackling climate change adaptation in existing buildings. Recently, focus for market activation in the construction sector has shifted towards dealing with the overhaul of the existing building stock. Article 9 of the EPBD (European Union 2010) brings in refurbished buildings under

the near zero-energy umbrella by requiring member states to develop policies in order to stimulate the transformation of refurbished buildings into near zero-energy buildings (NZEB). The Irish National Energy Efficiency Action Plan 2013-2020 (DCENR 2013) report has identified refurbishment of existing public sector buildings as a key focus. The report states that there are over 10,000 existing public sector buildings in Ireland and a key strategy for delivering retrofit projects may be through Energy Performance Contracting. Cork Institute of Technology (CIT) have recently completed a pilot project for a low energy retrofit of their existing 29,000m^2 teaching building constructed in 1974. The retrofit pilot covered 1.5% of the total building floor area. The project scope consisted of design and installation of a structurally independent external envelope solution. O'Sullivan et al (O'Sullivan et al. 2013) have summarised details of the design and specification of the retrofit solution. In this paper work is summarised from experimental measurements of ventilation rates under different ventilation opening configurations in a single sided isolated office space within the retrofit. The objective is to investigate whether modification in both the building thermophysical properties and ventilation opening design has influenced ventilation rates and the internal environment and under what conditions is performance enhanced. A control space in the existing building has been identified and utilised for comparative purposes.

Figure 1: The recently completed retrofit pilot project at B-Block CIT (a) retrofit space (b) control space

Section 3 of the paper summarises details regarding the existing building, completed retrofit strategy, natural ventilation system and operational configurations. Section 4 provides information about the ventilation rate (ACH^{-1}) tests including experiment setup, results and analysis. Sections 5 summarises findings from comparative studies of the internal environment in the control space and retrofit space. Results are categorised according to the four configurations detailed in section 4.2.
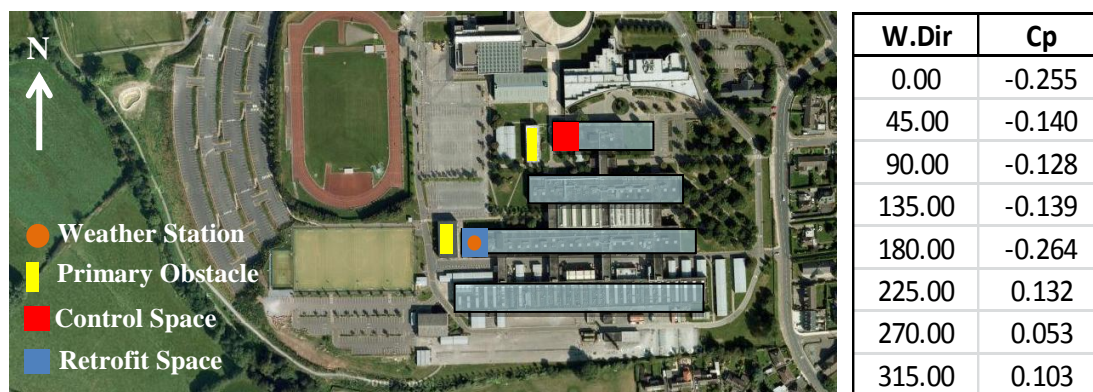

W.Dir	Cp
0.00	-0.255
45.00	-0.140
90.00	-0.128
135.00	-0.139
180.00	-0.264
225.00	0.132
270.00	0.053
315.00	0.103

Weather Station
Primary Obstacle
Control Space
Retrofit Space

Figure 2: Site Location of Control and Retrofit Space & associated surface wind pressure coefficients, C_p

2   LOCAL CLIMATE (2013 & LONG TERM)

Ambient air temperature, solar radiation and wind speed 95th Percentile values for May – September 2013 are presented in Table 1. Cork Airport TMY3 data also shown for comparison and was generated using Meteonorm 7 software []. Weather data used for the analysis in this paper was obtained from a weather station located on the roof of the retrofit

space, set 6.0m in from the edge of the building and at an elevation of 8.0m above the finished roof level.

Table 1: Local Climate at CIT

Month	Cork Airport TMY3 95th Percentile			Summer 2013 95th Percentile**		
	G_h (Wh/m^2)	T_a (°C)	WS (m/s)	G_h (Wh/m^2)	T_a (°C)	WS (m/s)
May	742	17.2	10.0	730	16.0	6.3
June	815	19.5	9.3	826	20.6	5.0
July	707	20.7	9.0	795	25.0	4.3
August†	662	20.0	9.3	567	19.1	4.7
September*	574	19.4	9.0	-	-	-

† Data up to 15th August only for short term; *Data not yet available for short term; **Data taken from zero2020 weather station

3   DESCRIPTION OF CONTROL SPACE & LOW ENERGY RETROFIT

3.1 Envelope Components

The external envelope retrofit solution involved the installation of a new external façade, independently supported at the base and tied into the structure at certain locations. The solution can be sub-divided into three broad modular categories; Roof module, opaque wall module and the fenestration module comprising both the glazing and ventilation openings. O'Sullivan et al (O'Sullivan et al. 2013) have already outlined in some detail the component specifications elsewhere. Figure 3 below provides information on the final wall build up and external retrofit solution applied. It should be noted that the entire existing structure has remained in place as part of the solution. The main thermophysical properties for the existing building and the retrofit components are summarised in table 1.

Table 2: Thermophysical properties of opaque external retrofit solution & fenestration module

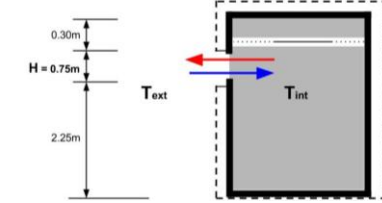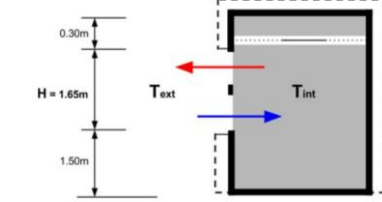|	Description	Dim. (mm)	Location	ω/φ (W/mK) / h	f (W/mK)	U_{wall} (W/m^{2}K)	$U_{fenestr.}$ (W/m^{2}K)
1	Existing Internal Block	100	Control Space	5.49 / 1.017	0.608	3.633	6.0
2	BASF Wall-tite Spray Foam	86					
3	Existing aggregate panel	125					
4	Air gap	30					
5	Kingspan benchmark ceramic granite panel	12	Retrofit Space	5.92 / 0.963	0.004	0.090	0.84
6	Kingspan support rail	37					
7	Kingspan KS 1100 insulated panel	125					
8	AMS support mullion	125					
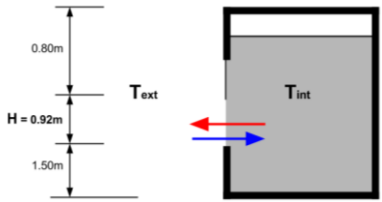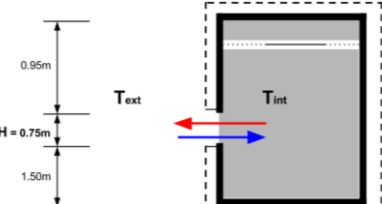
Figure 3: (a) Opaque Retrofit module, (b) fenestration module (including ventilation inlets)

3.2 Ventilation System

For most enclosed spaces in the existing building the ventilation system is based on single sided top hung pivoting window sections. There is generally one opening window per structural grid. These are the original 1974 windows. In the retrofit space fenestration system, the ventilation module uses a flush faced external louvre with individual air inlet sections.

Inside this louvre ventilation is supplied using dedicated insulated doors controlled either manually or automated based on conditions in the enclosed spaces (see Table 3). The overall thermal transmittance performance of this unit including doors and linear transmittance is 0.84 W/m^2k, according to IS EN 10077-2:2003 (NSAI 2012). The new fenestration module resulted in an overall opaque/transparent area ratio reduction of 20%. Unwanted ventilation through adventitious openings has also been greatly reduced. The retrofit envelope air permeability was tested in accordance with BS EN 13829:2001. The envelope achieved an air permeability of 1.76 $(m^3/hr)/m^2$ at 50Pa building pressure. The existing structure was measured as 14.77 $(m^3/hr)/m^2$. Details of the different ventilation opening configurations including are highlighted in Table 3 below.

Table 3: Summary of ventilation opening data & operating configurations

Location & Information	Configuration & operating mode	Vent Opening Type	A_{eff} A_{eff}/A_w	Schematic Envelope Flow Model
Existing building First Floor D-Block Single office Room D259 *(Control Space)*	CS/1.0/M		0.32 m^2 3.7%	
Retrofit building First Floor B-Block Single Office West Facing Room FF-03 *(Retrofit Space)*	RE/2.0/M		0.21 m^2 2.4%	
	RE/3.0/A		0.21 m^2 2.4%	
	RE/4.0/M/A		0.42 m^2 4.9%	

CS=Control Space; RE = Retrofit Space; M = Manual; A=Automated with manual override

4   VENTILATION RATE (ACH^{-1}) MEASUREMENT

4.1 Tracer Gas Concentration (TGC) Decay technique

The ventilation rate for the control space and retrofit space was measured using a single zone TGC decay technique. TGC decay techniques are among the most efficient to assess airflow patterns within buildings. They consist of 'marking' the air with a tracer gas (Roulet, 2007). Carbon Dioxide (CO_2) was chosen as the tracer gas for this work due to the ease of use, availability of analysis equipment, its density being similar to air and cost. CO_2 qualities as a tracer are summarised in Table 7.2 of Roulet (Roulet 2007). One main concern when using CO_2 as a tracer gas can be the presence of a large background concentration and, if constant, account must be taken for this in analysis of data by substituting the difference between

indoor and outdoor concentration for indoor concentration in the analysis (Persily 1997). For each of the tests presented in this work outdoor CO_2 concentrations during the test and indoor zone CO_2 concentrations prior to the test start were monitored and test start time concentration levels adjusted accordingly. Overall average outdoor CO_2 concentration during testing (as a percentage of the indoor concentration for each configuration) are summarised in Table 4. Occupant generated CO_2 if present in the zone during the test must also be accounted for in the analysis. Occupant CO_2 generation rates were calculated using ASHRAE Fundamentals (ASHRAE 2009). Based on specific information relating to the occupant the volumetric generation rate of CO_2 was calculated according to

$$Q_{O_2} = {}^{MA_D}\!/\!_{21(0.23RQ + 0.77)} \tag{1}$$

Where Q_{O_2} is the volumetric consumption rate, RQ is the respiratory quotient and gives the ratio of CO_2 generation to O_2 consumption, (taken as 0.83); M is the metabolic rate in W/m^2 and A_D is the DuBois surface area (calculated as $02.02m^{0.425}l^{0.725}$). Where an occupant was present in the zone, the occupant generation rate was assumed to be constant during the test period and I_{occ} was to be incorporated into the concentration mass balance equation where I is the injection rate of a particular source (kg/s). For the TGC decay technique a suitable quantity of tracer gas is injected to achieve a measureable initial concentration, $C_{initial}(t_0)$. After the initial pulse injection period, the injection is stopped and $I_{pulse} = 0$,. Once the pulse injection has stopped the tracer gas is then mixed within the zone until the average uniformity concentration difference for the test reaches an acceptable level. The tracer gas is then monitored using a gas analyser from the test start time until the test end time, in this instance once the concentration has returned at or close to the pre-test concentration levels. Based on Sherman (Sherman 1990) by solving the continuity equation for tracer gas it can be found that tracer gas concentration decays with time according to:

$$C = C(t_0) e^{(-Nt)} \tag{2}$$

And Including occupant generated CO_2 during the test the average N can be calculated from:

$$N = \frac{1}{T} \ln \left(\frac{C_{final}}{C_{initial}} \right) - \left(\frac{I_{occ}}{C} \right)$$

4.1 Experiment setup and Test conditions

35 TGC Decay tests were completed in total. Table 4 outlines the breakdown of tests completed for each operational configuration. Tests were completed in accordance with the procedure set out in ASTM E741-11 (2011). Two tracer gas sampling locations were used within the zone being tested. A single injection point was used. This was a standard CO_2 cylinder and heated flow regulator. CO_2 concentration analysers were AlphaSense IRC-A1 Non Dispersive Infra-Red (NDIR) Sensors. As CO_2 is denser than air ($\sigma = 1.53$) the gas was actively mixed as it entered the space. A maximum 10% acceptable uniformity of concentration criteria between both sampling locations in accordance with ASTM E741-11 was used to determine when there had been sufficient mixing. Figure 4 describes the equipment layout for both the control space tests and retrofit space tests.

Table 4: Schedule of experimental tests and conditions

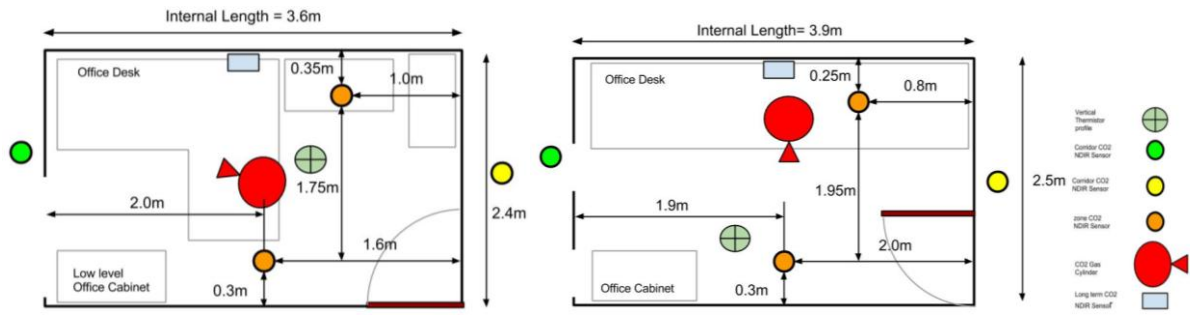| Config.	No of tests	Range of test durations	Average Conc. uniformity	Start PPM Range (Adj.)	End PPM Range (Adj.)	Average B.G. PPM (%)
CS/1.0/M	13	24 – 90 min	5.11 %	2776-5743	386-1286	10.3
RE/2.0/M	6	26 – 77 min	3.10 %	3129-4687	495-1583	12.3
RE/3.0/A	3	31 – 50 min	3.47 %	3105-3787	865-1424	13.4
RE/4.0/A/M	13	30 – 161 min	4.73 %	2546-4198	334-1179	13.0

Figure 4: TCG Decay test equipment locations (a) control space (b) retrofit space

The time period of each test varied based on the configuration. Figure 5 shows results from two of the tests showing three stages; injection, mixing and stabilisation of concentration and concentration decay rate.
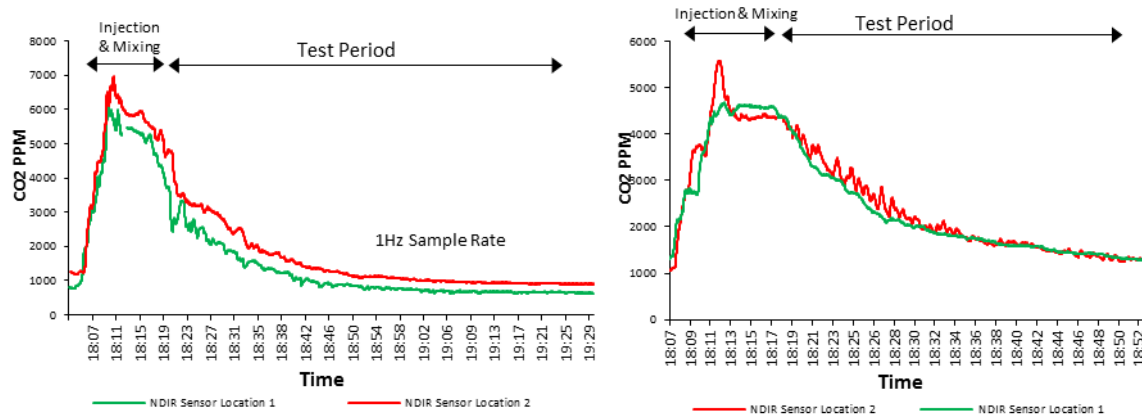

Figure 5: PPM Profile for TGC Decay Test (a) 12 RE/4.0/A/M & (b) Test 26 CS/1.0/M

4.2 Results & Analysis

Table 1 contains summary data regarding the 35 tests. Having measured the ventilation using the TGC decay technique the purpose of the investigation was to understand whether the dominant forces were different for the different configurations under similar conditions. The highest range of ACH^{-1} can be seen to occur in the control space. It produced the highest ACH^{-1} and on average had higher ACH^{-1} under similar conditions.

Table 5: ACH^{-1} Controlled Test Results Overview

Test Config.	Max ACH^{-1}	Min ACH^{-1}	Std. Dev.	Ave ACH^{-1}	Occ. < 3.0 ACH	Occ. < 1.5 ACH	WS Range (m/s)	No. of Windward/ Leeward tests	ΔT_{ie} Range
CS/1.0/M	4.70	1.16	1.19	2.81	7	4	1.41-5.20	9/4	4.2-8.9
RE/2.0/M	3.59	1.28	0.89	2.14	1	2	1.36-5.24	4/2	0.5-5.5
RE/3.0/A	2.75	1.13	0.89	1.73	0	2	3.33-4.24	1/2	1.1-5.3
RE/4.0/A&M	3.70	0.54	0.94	2.52	5	3	1.52-4.47	7/6	0.4-7.1

Envelope temperature differences were generally higher for the CS tests. Under each of the three configurations in the RE space there is a large variation in ventilation rate with average ACH^{-1} generally less than 2.0 ACH^{-1} for Config RE/2.0/M & RE/3.0/M. For the full height configuration RE/4.0/M/A, 40% of tests were above 3.0 ACH^{-1}. Overall these are still low ventilation rates and will impact on the thermal time constant, heat transfer to and from the structure and indoor air freshness. The retrofit space had lower ACH^{-1} than the control space potentially due to reduced wind effect from the flush faced louvres and reduced temperature differences. The two main forces that can give rise to ventilation rates are stack effect, generated by temperature difference across the building envelope and pressure at the building

surface due to wind effect (magnitude and direction). Single sided ventilation rates due to these combined forces can be described using a number of semi-empirical models. Warren (1978) proposed 2 separate correlations for stack and wind effect, taking the larger of the two to quantify ventilation rate. Dascalaki (1996) proposed an alternative correlation to take account of wind effects. More recently Larsen and Heiselberg (Larsen & Heiselberg 2008) proposed a more complex correlation that takes account of the thermal effects, wind speed & direction. Larsen & Heiselberg found that the dominating force differs between wind speed and ΔT_{ie} depending on the ratio between these forces and the wind direction. Based on this further analysis of the results above is needed. In attempting to quantify these combined forces, Warren (1978) proposed the use of 3 dimensionless values in order to study the strength of stack effect in contributing to the ventilation rate in single sided ventilation. The Archimedes number, $Ar = (Gr/Re^2)$ is a measure of the relative strength of buoyancy and inertia forces described as:

$$Ar^{0.5} = \frac{\Delta T g H}{T v_{wind}^2} \tag{3}$$

By plotting the Archimedes number as a function of Flow number, F, it is possible to see whether stack effect or wind effect is dominant for each measured ventilation rate.

$$F = \frac{q ACH}{A_{eff} v_{wind}} \tag{4}$$

The use of a flow number due to thermal stack effect alone, F_{th}, is introduced to the plot. K is a function of opening discharge coefficient and depending on whether an orifice law or quadratic law is used K will vary. We have taken K= 0.2 (based on a $C_d = 0.61$) for the opening

$$F_{th} = K.Ar^{0.5} \tag{5}$$

The Warren chart in figure 6 suggests that for a large number of the tests the ventilation was either equal to or less than the stack ventilation rate.
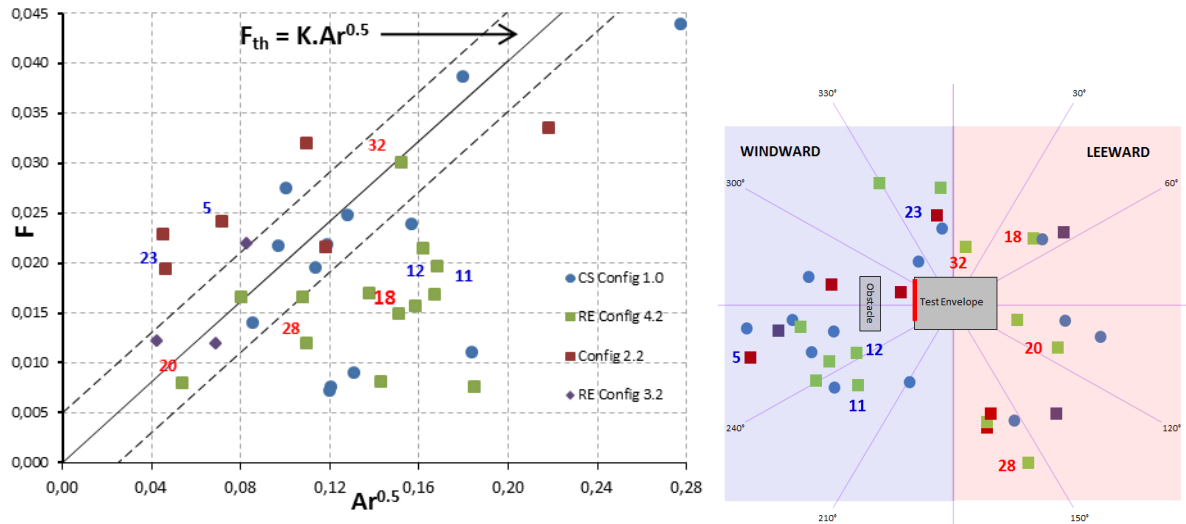

Figure 6: Warren Plot & Wind Direction/Wind Speed for each test categorised according to configuration

Figure 6 also contains a plot showing wind direction and magnitude for each of the tests, colour coded according to configuration. Some test values have been numbered according to the test reference. Blue represent windward and red leeward tests. It is clear from the results shown that both windward and leeward directions are opposing stack effect for RE/4.0/A/M and all test results are at or below stack ventilation rates. Where there is leeward winds these were with ΔT_{ie} values of 0.4°C - 4.4°C. Caciolo et al (Caciolo et al. 2011) reported that from experimental tests of single side ventilation at low wind speeds stack effect was more dominant creating turbulence at the opening. Test 11 & 12 had windward conditions but wind

speeds were relatively low. A Recirculation zone is likely present for leeward tests with no mixing layer thus reducing wind effect on ACH[-1]. For RE/2.0 the low height dimension suggests stack effect wasn't sufficiently established across opening and wind effect was more dominant.

5 INTERNAL ENVIRONMENT

5.1 Zonal Thermal Stratification

According to Etheridge (2011) while stratification has practical importance in that it affects envelope flows it is not as important as the mean temperature of air and surrounding surfaces, i.e. if these temperatures are outside an acceptable range then stratification is of secondary importance. However it can be viewed as a source of uncertainty when modelling zone ventilation and temperatures and using a single node technique and some understanding of the likely effects should be established. Li (2002) proposes three possible "good" profiles for vertical air temperature profiles; linear, a two layer profile & a mixed profile. A simple linear temperature profile can be described using the following Kappa model (BSim2000) which uses a k function for varying gradients of stratification, $k = T_f - T_o / T_R - T_o$.:

$$T = T_0 + (T_R - T_0)\left(\frac{z}{H}(1 - k) + k\right) \tag{6}$$

Li (2002) also stated that the effect of thermal stratification on airflow can be very significant and ignoring it can lead to significant under estimation of the neutral levels in a building. In un-insulated or poorly insulated buildings stratification may also affect heat transfer between inside air and walls, modifying ventilation flow rates. In order to investigate what level of thermal stratification was present in the existing building and how the retrofit strategy has modified this vertical temperature profile was measured during each of the ACH[-1] tests and for an extended period covering 9th June 2013-23rd July 2013. This data was useful for studying stack driven ventilation rate and analysing the conditions that result in higher stratified air than normal in each zone. It can assist in quantifying the uncertainty in air temperature prediction when using multi zone airflow networks models for existing and low energy retrofit buildings. Comparison of stratification profiles for retrofit configurations are presented in figure 7. Figure 8 shows the effect of high external temperatures & night cooling for the retrofit space. The data was obtained during a particularly warm period with external temperatures reaching 10 year highs. Etheridge (2011) mentions the use of the dimensionless stratification factor (*StrFr*) to also characterise its relative strength in a single zone compared to envelope temperature difference:

$$\frac{\Delta T_s}{\Delta T_{ie}} = \frac{T_H - T_o}{T_{H/2} - T_E} \tag{7}$$

Both these values have been calculated and tabulated for ACH[-1] tests that were highlighted as being stack dominant in the Warren plot in section 4 above. Longer term *StrFr* are also shown in table 7 below.

5.2 Instrument setup

Hanwell Radio-logger RL4000 wireless data loggers and precision thermistors with an accuracy of +/- 0.1°C between -25°C to 50°C were used for vertical temperature distributions. Measurements were recorded every 10 minutes in the retrofit space and every 5 minutes in the control space. Measurements were taken at 8 vertical positions from floor to false ceiling level spaced evenly throughout the 3.2m height. Surface and air temperatures are continuously logged using Gemini Tiny-tag data loggers.

5.1 Results & Analysis

Figure 7 highlights vertical temperature profiles for the RE configurations. Note these have differing opening heights. They are plotted for similar *StrFr* in (a) and the largest test value in

(b) (same relative strength). RE/4.0/A/M demonstrates the largest temperature gradient in each case though RE/3.0/A is very similar in (b).
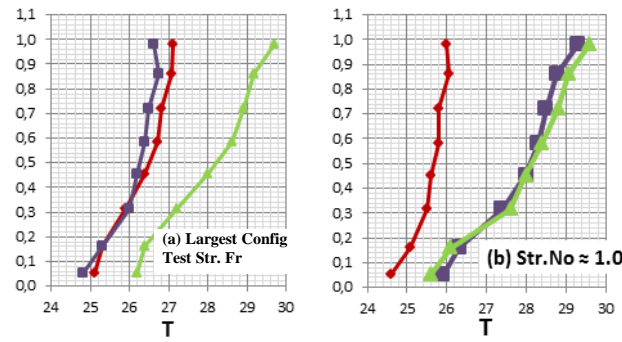

Figure 7: Vertical Stratification RE config during ACH Tests 16, 23, 20 (colour as per Config)

Table 6 below summarises the vertical temperature gradients, kappa values and *StrFr* for each test that was seen to have stack dominated ventilation flow based on Warren plot results earlier. All CS tests that demonstrated strong stack effects have small stratification numbers while the opposite is the case for the RE space. This indicates that in the CS ΔT_{ie} was always stronger than ΔT_s and suggests stratification is potentially of secondary importance (other than affecting heat transfer at the zone surfaces) to envelope flows. In the RE space, although T_{int} was generally lower and ΔT_{ie} & ΔT_s both individually lower than the CS, results suggest stratification may still play a significant role in the thermal dynamics of the internal zone.

Table 6: Stratification Profiles for Stack Dominated Tests based on Warren plot

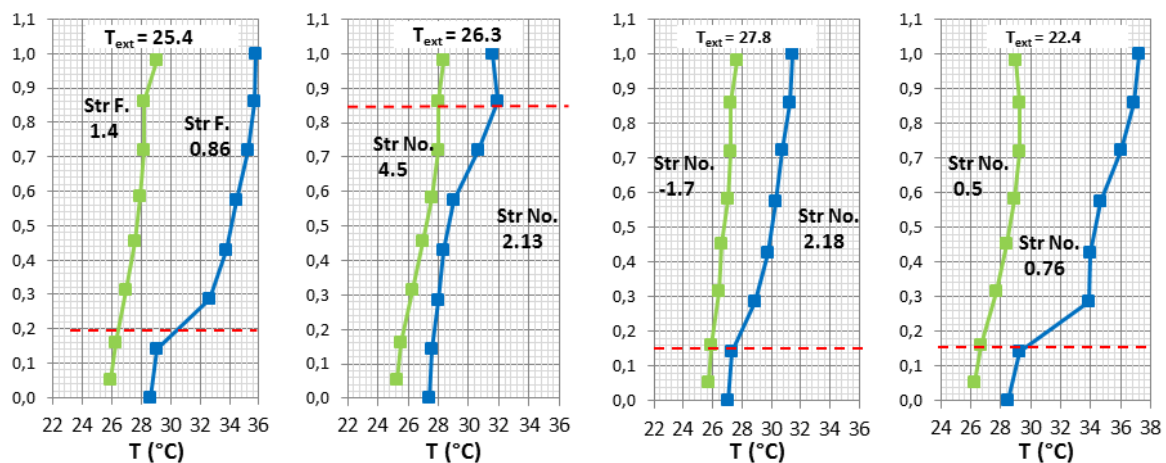| Location/Config	Test	*StrFr*	$|F-F_{th}|$	Km^{-1}	Kappa Range
CS/1.0	3	0.227	0.002	0.49	0.95
CS/1.0	4	0.551	0.002	0.94	0.76
CS/1.0	27	0.565	0.001	1.00	0.72
CS/1.0	2	0.621	0.003	1.81	0.64
RE/2.0	29	0.700	0.002	1.30	0.57
CS/1.0	14	1.051	0.003	3.20	0.38
RE/3.0	25	1.111	0.002	1.20	0.31
RE/3.0	16	1.125	0.004	0.60	0.13
RE/4.0	32	1.438	0.001	0.80	0.01
RE/4.0	24	1.809	0.000	1.20	0.01

Figure 8: RE vs. CS stratification for (a) 10-Jul 16:45 (b) 12-Jul 15:30 (c) 13-Jul 16:50 (d) 18-Jul 20:00

Considering some specific dates, 10th July had night cooling (NC) activated in RE and blinds fully closed but no NC in CS; 12th July had NC activated in RE and CS with blinds in RE fully closed and CS internal blinds 50% closed; 13th July is a Saturday with window open 24hrs in CS but only RE/3.0/A Config active all weekend in RE space. 18th July had NC in

both spaces. On 10th July even though there's a high ΔT_s it still isn't more dominant than ΔT_{ie} and less significant, while the RE space has a lower temp diff but a StrFr > 1. Night cooling resulted in mean zone temp 2.5K above T_{ext} but outside acceptable ranges. On 12th July *StrFr* is very strong in RE mainly due to ΔT_{ie} but again suggests the vertical temperature profile is important to understanding ventilation coupling with thermal mass at different heights (WS = 2.7 ms^{-1} WD = parallel to envelope 196°). T_{ext} on 13th July is one of the highest recorded during the summer 2013 period and *StrFr* for RE space is -1.7, ($T_{int} < T_{ext}$).

Table 7: 20th June – 19th July 2013 Percentile Values *Str.Fr ($\Delta T_s/\Delta T_{ie}$)* Data

Space.	Occupied hours (09:00-18:00)				Unoccupied Hours (18:00-09:00)			
	50th	75th	95th	% occ hrs >1	50th	75th	95th	% occ hrs>1
Control	0.411	0.691	1.19	9.0%	0.192	0.333	0.622	0.0%
Retrofit	0.202	0.609	2.59	14.5%	0.157	0.290	0.611	2.2%

Table 7 shows how stratification is substantially reduced during overnight periods. The 95th percentile value for unoccupied hours of 0.611 is largely based on conditions up to around 21:00 each evening where there is still significant stratification. Both spaces monitored are west facing and this suggests an association with incident solar irradiation and the occurrence of peak conditions later in the evenings. Most of the peak conditions take place at this time even though peak day time air temperatures occur as early as 11:45. The retrofit occupied hours 95th percentile value of 2.59 does highlight that there is stratification still present in the space and it has a significant relative strength compared to ΔT_{ie}. Temperatures at the surface of the exposed roof slab are often 2-3°C higher than would be reported based on a mid-level zone thermostat which can be significant in ventilate cooling of a low energy space.

5.2 Thermal time constant & T_{int} time lag

While the envelope structure has undergone a major external material upgrade with a significant reduction in decrement factor (0.608 to 0.004) the internal thermal mass in contact with the zone air has largely remained unchanged other than part exposure of the roof slab in the retrofit though perforated ceiling tiles. It should be noted there is also a difference in quantity of thermal mass between CS and RE with CS only having one internal block-work wall while RE has two. The zone thermal time constant described below, is plotted for each ACH^{-1} test result as a function of flow number, *F*, shown in figure 9.

$$\tau = \left[(\rho C_p Vol)_{air} / (\rho C_p Vol)_{mass} \right]$$ (8)

Higher τ values are seen in the RE, even a similar F values. Table 8 presents a comparison of daily maximum & minimum internal temperatures for RE & CS with the corresponding hour of occurrence for 8th – 14th July 2013. If NC was present on the previous night this is indicated by the symbol (*Config RE/4.0/M/A & ** Config RE/3.0/A) adjacent to Max T_{int}.

Table 8: Measured $T_{H/2(peak)}$ Time Lag during week 8th-14th July 2013

Day	External		RE				CS			
	Max T_{ext} (°C)	Occ. (hr)	Max T_{int} (°C)	Occ. (hr)	Min T_{int} (°C)	Occ. (hr)	Max T_{int} (°C)	Occ. (hr)	Min T_{int} (°C)	Occ. (hr)
8th	25.4	16:35	29.0	18:50	24.4	06:00	36.8	19:35	25.0	05:40
9th	27.1	14:40	28.6	18:40	25.5	23:40	36.1	19:00	26.8	07:05
10th	26.4	13:00	29.1*	19:50	22.8	07:10	36.5	19:25	28.0	06:10
11th	23.9	11:45	30.0*	18:40	22.8	06:50	-*	-	25.0	07:40
12th	26.4	15:15	28.0*	19:00	22.0	06:30	35.6*	17:35	-	-
13th	27.8	14:20	28.4**	18:40	25.1	06:20	36.1*	17:45	24.3	07:45
14th	25.8	16:55	27.9**	20:00	25.8	07:20	33.9*	17:20	25.7	23:40

Table 9: $T_{H/2}$ Peak Daily Air Temperatures and Diurnal Variation (20th June – 19th July 2013)

Space.	hrs>25°C (%Σhrs)*	hrs>28°C (%Σhrs)*	95th Perc. $\Delta T_{ext(24hr)}$	50th Perc. $\Delta T_{ext(24hr)}$
Control	34	17		
Retrofit	33	3.5		

Based on 981 working hours May-September
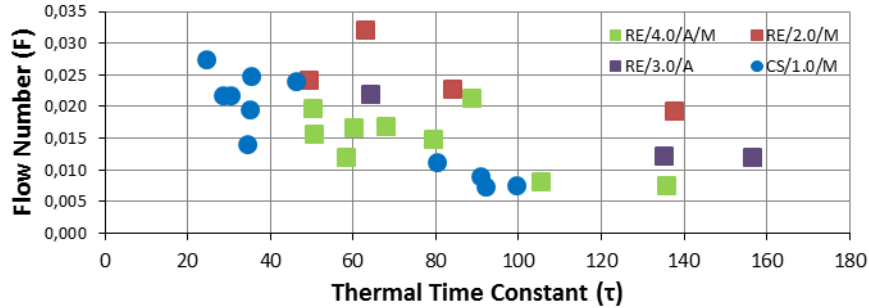
Figure 9: τ vs. F based on each controlled ACH^{-1} test

6   CONCLUSIONS

While the current results and analyses are not yet definitive it is clear from current findings that the retrofit works have modified the internal environment and ventilation rate for isolated spaces with single sided ventilation. The largest ACH^{-1} rates measured in the retrofit space were still lower than the existing building under similar conditions. Error analysis and uncertainty of results also still needs to be quantified. The analysis suggests ventilation rates were either dominated by stack effect or lower than the rate due to stack effect indicating some counteracting force during these tests. More tests are needed to better understand how different forces affect ventilation performance in the RE, particularly for configurations RE/2.0/M & RE/3.0/A. In the CS when there were windward conditions with wind speeds > $4ms^{-1}$ these tests still displayed flow numbers very close to F_{th} ($\Delta T_{ie} > 6.5K$ in both tests). In the RE space leeward tests were generally stack dominant or lower. However, there were results that had flow numbers very close to F_{th} with both high and low wind speeds and windward and leeward conditions. This suggests that the influence of wind conditions on ventilation rates is complicated by local obstacles at the site nearby the CS and RE spaces. More analysis and additional testing is required to establish to what extent wind conditions are affecting ventilation rate. What is clear is for configuration RE/4.0/A/M, which is the proposed summer cooling arrangement; nearly all measurements of ventilation rate were lower than stack effect alone. Regarding Internal thermal environment, this has been modified with the mean zone temperature substantially reduced. Diurnal temperature amplitude has also been reduced. This is as expected. ΔT_s had a lower magnitude in the RE but had higher *StrFr* values suggesting it had a higher relative strength compared to the existing building. Night cooling didn't appear to have a measurable influence on the RE space which may be due to low ventilation rates at night, something that may need to be studied further. In the CS when night cooling was used $T_{int(max)}$ magnitude didn't change but the hour of occurrence shifted back to earlier in the day. This is probably due to ventilating the space in the evening time when high solar gains are present as opposed to the night cooling, although $T_{int(min)}$ were moderately reduced.

7   ACKNOWLEDGEMENTS

8   REFERENCES

ASHRAE, 2009. *2009 ASHRAE HANDBOOK - Fundamentals*,

ASTM E741-11 (2011), 'Standard Test Method for Determining Air Change in a Single Zone by Means of a Tracer Gas Dilution'.

Caciolo, M., Stabat, P. & Marchio, D., 2011. Full scale experimental study of single-sided ventilation : Analysis of stack and wind effects. *Energy & Buildings*, 43(7), pp.1765–1773.

Dascalaki (1996)

DCENR, 2013. *Irelands Second National Energy Efficiency Action Plan*,

Etheridge, D. (2011). Natural Ventilation of Buildings: Theory, Measurement and Design ISBN: 978-0-470-66035-5, Chapter 6 - Internal air motion, zonal models and stratification. 180-183

European Union, 2010. Directive 2010/31/EU. , pp.13–35.

Kolokotroni, M.,Webb, B.C. and Hayes, S.D. (1996b)'Summer cooling for office-type buildings by night ventilation' in Proceedings of the 17th AIVC Conference on Optimum Ventilation and Air Flow Control in Buildings, Gothenburg, Sweden, 17-20 September, vol 2, pp591-599

Kolokotroni M., Watkins R., Santamouris, M., Niachou, K., Allard, F., Belarbit, R., Ghiaus, C., Alvarev, S. and Salmeron, J.M. (2002)'Lissen: Passive ventilation cooling in urban buildings: An estimation of potential environmental impact benefits', in Proceedings of the EIPC 2002 Conference, Lyon, France

Larsen, T.S. & Heiselberg, P., 2008. Single-sided natural ventilation driven by wind pressure and temperature difference. *Energy and Buildings*, 40(6), pp.1031–1040.

Li, Y. (2002) ' Integrating thermal stratification into natural and hybrid ventilation analysis' Technical Report TR15, IEA-ECB&CS Annex 35, pg1-38

NSAI, 2012. ISO 10077-2:2012 Thermal performance of windows, doors and shutters - Calculation of thermal transmittance - Part 2 : Numerical method for frames,

O'Sullivan, P. et al., 2013. Design and Performance of an External Building Envelope Retrofit Solution For a Grid Optimised Concrete Structure: A Case Study. In *IMC30 Conference Proceedings 2013*.

Persily, A. (1997) 'Evaluating Building IAQ and Ventilation with Indoor Carbon Dioxide', ASHRAE TRANSACTIONS 1997, V.103, Pt 2

Roulet, C.A., (2007). Ventilation and Airflow in Buildings: Methods for Diagnosis and Evaluation, BEST (Buildings Energy and Solar Technology). Chapter 7 - Common methods and techniques, pg 133

Sherman, M., 1990. Tracer Gas Techniques for Measuring Ventilation in a Single Zone. *Building and Environment*, 25(4), pp.365–374.

Warren, P.R., 'Ventilation through openings on one wall only'. Proceedings of the International Centre for Heat and Mass Transfer Conference - 'Energy Conservation in Heating, Cooling and Ventilating Buildings, Dubrovnik, August 29 - September 2, 1977. Volume 1, pp 189-206. Publ. Hemisphere Publishing Corporation, Washington.

List of figures and tables